

Microwave Discharge Ion Thruster using Argon as a Propellant

IEPC-2007-205

Presented at the 30th International Electric Propulsion Conference, Florence, Italy
September 17-20, 2007

Makoto Miyoshi^{*}, Naoji Yamamoto[†], and Hideki Nakashima[‡]

Department of Advanced Energy Engineering Science, Graduate School of Engineering Sciences, Kyushu University,
6-1 Kasuga-kouen, Kasuga, Fukuoka Prefecture, 816-8580, Japan

Abstract: Thrust performances in a microwave discharge ion thruster using argon as a propellant were investigated. First, the ion beam current with magnetic configuration, which has two magnetic tracks on the base, was measured. The ion beam current with argon propellant is smaller than that of xenon for given incident microwave power. This would be due to its lower ionization potential. Next, the ion beam current with magnetic configuration, which also has two, but one is on the base and the other is on the side, was measured. The ion beam currents with argon are larger than those with xenon propellant at $P_i > 24$ W. This would be due to the difference of electrons energy. Since the frequency that electrons cross through the ECR layer is different between the two gases, because of the different mean free path. The thrust performance obtained is as follows ; the propellant utilization efficiency and ion beam production cost were 50% and 440 W/A, respectively at 2.45 GHz microwave input power of 37 W and argon gas flow rate of 2.28 sccm.

Nomenclature

e	=	electronic charge
g	=	acceleration of gravity
F	=	thrust
I_b	=	extracted ion beam current
I_{sp}	=	specific impulse
m_i	=	ion mass
\dot{m}_i	=	mass flow rate for ion source
P_i	=	incident microwave power
P_r	=	reflected microwave power
V_b	=	beam voltage
α	=	ratio of doubly charged ion current to singly charged ion current
ε_c	=	ion beam production cost
γ_T	=	thrust coefficient
η_t	=	thrust efficiency
η_u	=	propellant utilization
θ_b	=	beam divergence angle

^{*} Graduate student, Department of Advanced Energy Engineering Science, Kyushu University, makoto@aes.kyushu-u.ac.jp.

[†] Assistant Professor, Department of Advanced Energy Engineering Science, Kyushu University, yamamoto@aes.kyushu-u.ac.jp.

[‡] Professor, Department of Advanced Energy Engineering Science, Kyushu University, nakasima@aeskyushu-u.ac.jp.

I. Introduction

An ion thruster is one of the candidates for primary propulsion of deep space missions because it produces high thrust efficiency with a specific impulse of 3000-8000 s. Long lifetime is also required for deep space missions. A microwave discharge ion source would offer a potentially longer lifetime than a conventional electron bombardment-type ion source, since it would be free from contamination and degradation of electron emission capacity.^{1,2} Indeed, four 400 W thrusters are now being used as primary propulsion for a Japanese space probe "HAYABUSA" exploring an asteroid. It was launched on May 2003. And it succeeded in rendezvousing with the asteroid "Itokawa" in September 2005 and touching down on it in November 2005 after a 2-year flight. Now, HAYABUSA has already started on its return journey and is running to aim to reach the Earth in June 2010.³⁻⁵

For ion thrusters, the low ionization potential of the propellant is the better propellant, therefore, mercury, cesium, xenon, etc., have been used as a propellant. However, the activated gas, such as mercury and cesium, is not compatible with spacecraft due to its condensation and chemical reaction. Therefore, xenon has been the preferred propellant for ion thrusters because it is an inert gas, and because of its high propulsion efficiency due to its low ionization potential.

For deep space missions, the power supply that doesn't depend on the distance from the Sun is needed. Consequently, Nuclear Electric Propulsion System (NEPS), mounting nuclear reactor in space explorer and running electric propulsion system, would be adopted.⁶ The NEPS has some advantages on deep space mission because of its high thrust and high specific impulse, since it produce large amount of power that doesn't depend on the distance from the Sun. So, the priority of thrust efficiency becomes lower than that of specific impulse and cost. Therefore, argon would be better than xenon as a propellant due to low cost and enough supply, although the higher ionization potential of the argon results in an efficiency deficit. In addition, argon has some advantage in lifetime, since its sputtering yield is less than that of xenon when the specific impulses are the same.

The aim of this study is measuring the thrust performance in the microwave discharge ion thruster using argon as a propellant .

II. Experimental Set Up

The experimental apparatus is composed of microwave transmission system, evacuated system and ion engine. The frequency of microwave generator used is 2.45 GHz. A vacuum chamber of 60 cm diameter by 1 m length was used in these experiments. The vacuum apparatus has two rotary pump, a turbo molecular pump and a cryo pump. Argon gas (99.99%) and high-purity (99.999% pure) xenon gas was used as the propellant. To supply and control the propellant mass flow, mass flow controller (BROOKS 5850S) is used.

Figure 1 shows a 10 cm class microwave discharge ion thruster developed at Kyushu University.^{7,8} Emitted microwaves from the emitting antenna can be distributed to any antennas in the radial-waveguide. A receiving antenna can be set up in anywhere, and the distribution ratio of microwave power can be controlled by changing the antenna position, the length, and the diameter of the receiving antenna. The receiving antennas emit the microwaves

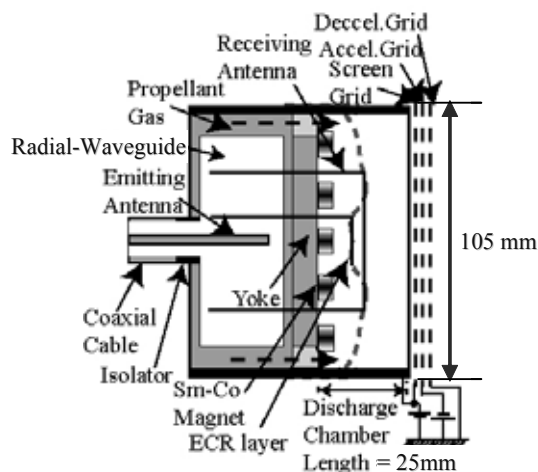


Figure 1. Microwave ion thruster developed at Kyushu Univ.

in the discharge chamber and the emitted microwaves heat electrons. The thruster itself can be insulated electrically from a microwave generator, since coaxial cable is insulated from radial-waveguide. So, the thruster can

Table 1 Grid parameter.

Parameter	Screen	Accel	Decel
Open area ratio, %	67	24	67
Hole diameter, mm	3.0	1.8	3.0
Potential, V	1,500	- 300	0
Thickness, mm	0.5	0.8	0.5
Material	Mo	Mo	C/C
Hole pitch, mm		3.50	
Grid gap, mm		0.5	
Number of holes		857	

reduce the number of parts and can be miniaturized. There would be little dissipation of the microwave power in the radial waveguide, since there does not exist standing waves by our numerical calculation.⁹ The diameter and the length of discharge chamber are 105 mm and 25 mm, respectively. The length of discharge chamber can be changed from 10 mm to 50 mm. Magnetic circuit is formed by samarium-cobalt (Sm-Co) permanent magnets and yokes which are made of soft iron. The antennas are made of Mo (1.5 mm in diameter). They are set on an electron cyclotron resonance (ECR) layer in a magnetic tube between the magnets, as shown in Fig. 2. A grid system for extracting ions from the discharge chamber is composed of a screen grid, an acceleration grid and a deceleration grid. The grid configurations are the same as that of Laboratory Model in MUSES-C.² The geometric parameters are shown in Table 1. The gap between the grids is 0.5 mm and the ion beam diameter is 105 mm.

A neutralizer was not used in this study, since there is little difference between the extracted ion beam current without a neutralizer and that with a filament neutralizer ($\phi = 0.2 \text{ mm} \times 100 \text{ mm}$, 2% thoriated tungsten).

III. Experimental Results and Discussion

In order to evaluate the performance of the ion engine, ion beam production cost, ϵ_c , propellant utilization, η_u , thrust, F , specific impulse, I_{sp} , and thrust efficiency, η_t are defined as,

$$\epsilon_c = (P_i - P_r) / I_B \quad (1)$$

$$\eta_u = \frac{I_b}{(e/m_i) \cdot \dot{m}_i} \quad (2)$$

$$F = \gamma_T I_b \sqrt{(2m_i V_b / e)} \quad (3)$$

$$I_{sp} = F / (\dot{m}_i g) \quad (4)$$

$$\eta_t = \frac{\gamma_T^2 \eta_u}{1 + \epsilon_c / V_b} \quad (5)$$

Considering the exhaust-beam divergence and the effect of doubly charged ion, γ_T is defined as,

$$\gamma_T = \cos \theta_b \times (1 + \alpha / \sqrt{2}) / (1 + \alpha) \quad (6)$$

α and θ_b are assumed to be 0.15 and 10 degrees, respectively.^{10,11} Thus, in this study, γ_T is estimated as $\gamma_T \approx 0.98 \times 0.96 = 0.94$

For the measurement of the ion beam currents, two magnetic configurations were used as shown in Fig.2. Configuration (1), which was shown in Fig. 2(a), has two magnetic tracks formed by three lines on the base yoke. Configuration (2), which was shown in Fig. 2(b), has two magnetic tracks formed by two lines of the Sm-Co magnet on the base yoke and one line on the side yoke due to expanded distance of magnetic tube.

Figure 3 shows the relation between incident microwave power and ion beam current in configuration (1). For $\dot{m} = 2.28 \text{ sccm}$, $P_i = 32 \text{ W}$, and $V_b = 1,500 \text{ V}$, the ion beam currents with xenon propellant and argon propellant are 85 mA, 64 mA, respectively. The ion beam current with argon propellant is worse compared to that with xenon propellant. This would be due to the difference in ionization cross section and neutral particle density between xenon and argon. Therefore, argon's ion production cost is higher than that of xenon, and ion beam current with argon propellant is smaller than that of xenon for given incident microwave power.

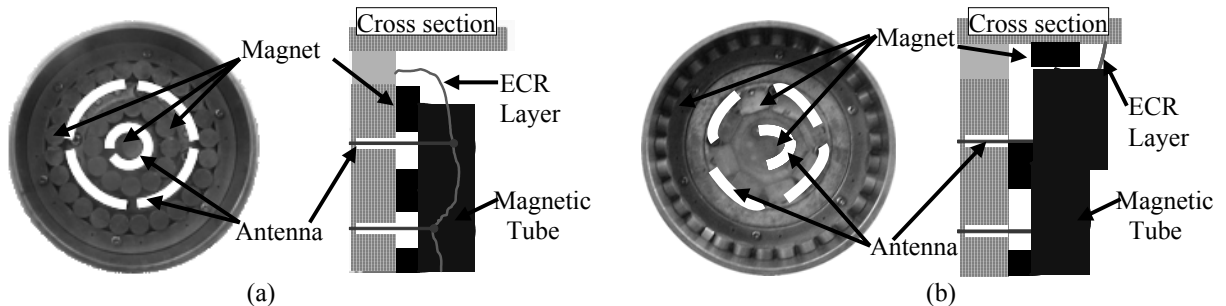


Figure 2. Magnetic configuration of ion engine.
(a) configuration (1), and (b) configuration (2)

Figure 4 shows the relation between incident microwave power and ion beam current in configuration (2). The ion beam currents with argon propellant are small compared to those with xenon below 24 W; the ion beam currents with xenon propellant and argon one are 65 mA, and 55 mA, respectively for $\dot{m} = 2.28$ sccm, $P_i = 21$ W, and $V_b = 1,500$ V. This tendency is similar to the previous one. However, ion beam currents with argon are larger than those with xenon propellant at $P_i > 24$ W; the ion beam currents with xenon propellant and argon one are 69 mA, and 77 mA, respectively for $\dot{m} = 2.28$ sccm, $P_i = 32$ W, and $V_b = 1,500$ V. This would be due to the following reason. That is, ionization can be occurred whole of the discharge chamber in argon, though it is not uniform in xenon. Figure 5 shows the picture of plasma emission in argon propellant and xenon propellant for $\dot{m} = 2.05$ sccm, $P_i = 32$ W, and $V_b = 1,500$ V. It can be observed that the emission from plasma is uniform for the entire area of the discharge chamber in the case of argon. However, the emission from plasma is not uniform in case of xenon. Intense emission can be observed only in the inner magnetic track. This would be due to the fact that the high energy electron exists only in the inner magnetic track in the case of xenon. For this thruster, propellant is injected through propellant gas supply port which is outside of 2nd magnetic track, as shown in Fig. 1. As a result, there are too much neutral gases in the outset magnetic tube, and they interrupt the electrons bouncing motion between the magnetic tube. Electrons obtain energy efficiently through the ECR layer in this type ion sources. Therefore, the chance that electrons pass through the ECR layer decreases as the collision rate increases due to decrease of mean free path. Therefore, ion beam current is saturated in this configuration.

On the other hand, in the case of argon, electrons can get enough energy whole over the discharge chamber, since less neutral density and smaller ionization cross section than xenon will not prevent electron energy gain processes. Therefore plasma emission from the discharge chamber is uniform. Though the ionization potential of argon is high, it can be compensated by high incident microwave power. Therefore, ion beam is increased with increase in the incident power. These results suggest that there are optimum magnetic tube lengths, i.e., the distances between magnet lines for variety of propellants and its densities.

Figure 6 shows the thrust performance for xenon propellant and argon propellant for $\dot{m} = 2.28$ sccm, and $V_b = 1,500$ V. The thruster performance for argon propellant with $P_i = 37$ W; propellant utilization efficiency, ion beam production cost, estimated thrust, estimated specific impulse and estimated thrust efficiency are 0.50, 440 W/A, 4.9 mN, 2,100 sec, and 0.34, respectively.

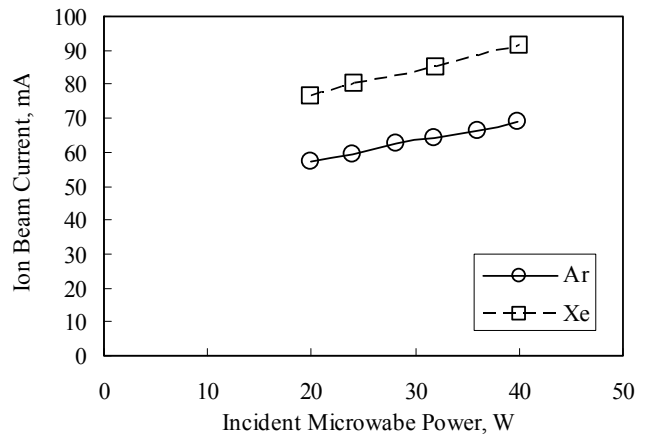


Figure 3. Influences of propellant with a configuration (1).

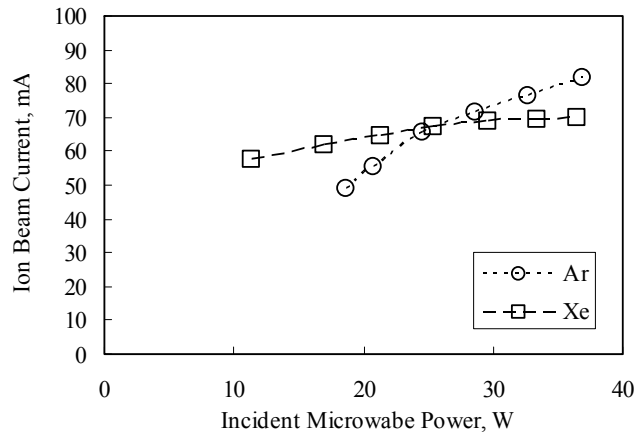


Figure 4. Influences of propellant with a configuration (2).

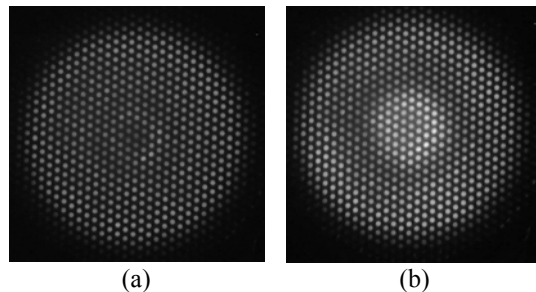


Figure 5. Pictures of plasma emission.
(a) argon propellant, and (b) xenon propellant
 $\dot{m} = 2.05$ sccm, $P_i = 32$ W, and $V_b = 1,500$ V

IV. Conclusion

In order to improve the thrust performance of a microwave discharge ion thruster, thrust performance with xenon and argon propellant was measured in two magnetic configurations. The conclusions are obtained as follows.

- 1) Thrust performance using argon as a propellant was improved by expanding magnetic tube. On the other hand, that using xenon was degraded. This result suggests that there are optimum magnetic tube lengths, i.e., the distances between magnet lines for variety of propellants.
- 2) We have achieved the following thruster performance using argon as a propellant; propellant utilization efficiency, ion beam production cost, estimated thrust, estimated specific impulse and estimated thrust efficiency are 0.50, 440 W/A, 4.9 mN, 2,100 sec, and 0.34, respectively., for $\dot{m} = 2.28$ sccm, $P_i = 37$ W, and $V_b = 1,500$ V.

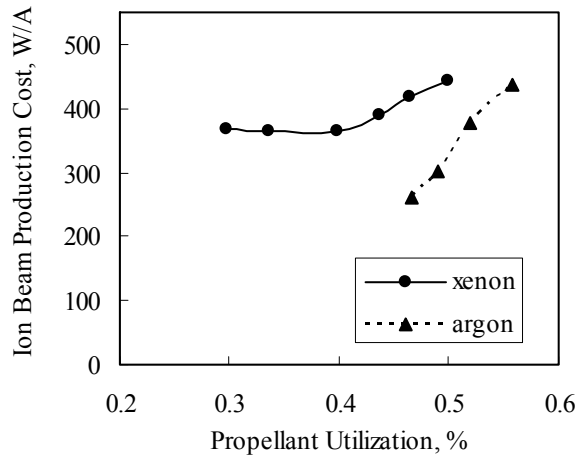


Figure 6. Thrust performance.
 $\dot{m} = 2.28$ sccm, and $V_b = 1,500$ V

Acknowledgments

The present work was supported by a Grant-in-Aid for Scientific Research (C)(2), No.16560691, sponsored by the Japan Society for the Promotion of Science.

References

- ¹Kuninaka, H., and Satoru, S., "Development and Demonstration of Cathodeless Electron Cyclotron Resonance Ion Thruster," *Journal of Propulsion and Power*, Vol. 14, No. 6, 1998, pp. 1022-1026.
- ²Funaki, I., Kuninaka, H., Toki, K., Shimizu Y., Nishiyama, K., and Horiuchi Y., "Verification Tests of Carbon-Carbon Composite Grids for Microwave Discharge Ion Thruster," *Journal of Propulsion and Power*, Vol. 18, No. 1, 2002, pp. 169-175.
- ³Kawaguchi, J., Uesugi, K., and Fujiwara, A., "The MUSES-C mission for the sample and return-its technology development status and readiness," *Acta Astronautica*, Vol. 52, 2-6, 2003, pp., 117-123
- ⁴A. Fujiwara, J. Kawaguchi, D. K. Yeomans, M. Abe, T. Mukai, T. Okada, J. Saito, H. Yano, M. Yoshikawa, D. J. Scheeres, O. Barnouin-Jha, A. F. Cheng, H. Demura, R. W. Gaskell, N. Hirata, H. Ikeda, T. Kominato, H. Miyamoto, A. M. Nakamura, R. Nakamura, S. Sasaki, and K. Uesugi, *Science*, **312**, 1330 (2006).
- ⁵Funaki, I., Kuninaka, H., and Toki, K., "Plasma Characterization of a 10-cm Diameter Microwave Discharge Ion Thruster," *Journal of Propulsion and Power*, Vol. 20, No. 4, 2004, pp. 718-726.
- ⁶M, S, El-Genk, editor, "A Critical Review of Space Nuclear Power and Propulsion, 1984-1993," *American Institute of Physics Press*, 1994
- ⁷Miyamoto, T., Yamamoto, N., and Hideki, N., "Development of a Microwave Discharge Ion Engine by Using Monopole Antennas," *Proc. of the 24th Int. Symposium on Space Technology and Science*, 2004, pp. 137-142.
- ⁸Miyamoto, T., Mii, K., Nishijima, T., Takao, Y., and Hideki, N., "Development of a New Microwave Discharge Type Ion Engine," *Vacuum*, **73**, 2004, pp. 391-396.
- ⁹Watanabe, T., Ogawa, M., Harada, T., and Nishikawa, K., "Mobile Antenna System for Direct Broadcasting Satellite," *R & D Review of Toyota CRDL*, Vol. 32, 1997, pp. 23-33 (in Japanese).
- ¹⁰Takegahara, H., Kasai, Y., Gotoh, Y., Miyazaki, K., Hayakawa, Y., Kitamura, S., Nagano, H., and Nanamura, K., "Beam Characteristics Evaluation of ETS-VI Xenon Ion Thruster," *Vacuum*, **73**, 2004, pp. 391-396.
- ¹¹Masui, H., Tashiro, Y., Yamamo, N., Nakashima, H., and Funaki, I., "Analysis of Electron and Microwave Behaviors in Microwave Discharge Neutralizer," *Transactions of the Japan Society for Aeronautical and Space Sciences* (to be published).
- ¹²Masui, H., Yamamo, N., Nakashima, H., and Funaki, I., "Analysis of Plasma Behavior in Microwave Discharge Ion Engine," *AJCPP Paper*, AJCPP-A2051, Jan, 2005.